2000

# VLBI Monitoring of 3C 279 at 22 and 43 GHz: 1991-1997

B. G. Piner
*Whittier College*, gpiner@whittier.edu

A. E. Wehrle

S. C. Unwin

A. C. Zook

W. Xu

*See next page for additional authors*

*Astrophysical Phenomena Revealed by Space VLBI*
*H. Hirabayashi, P.G. Edwards and D.W. Murphy (eds.)*

# VLBI Monitoring of 3C 279 at 22 and 43 GHz: 1991-1997

B.G. Piner[1], A.E. Wehrle[1], S.C. Unwin[1], A.C. Zook[2],
W. Xu[3] & A.P. Marscher[4]

[1] *Jet Propulsion Laboratory, California Institute of Technology, USA*
[2] *Department of Physics and Astronomy, Pomona College, USA*
[3] *IPAC, California Institute of Technology, USA*
[4] *Department of Astronomy, Boston University, USA*

**Abstract**

We present results obtained from VLBI monitoring of the relativistic jet in 3C 279 at 22 GHz from 1991 to 1997 (18 epochs), and at 43 GHz from 1995 to 1997 (10 epochs). Measured speeds for all detected components are presented. Component C4 has followed a nonlinear path out from the core, and the motion of this component is discussed in detail.

## 1 Introduction and Observations

The blazar 3C 279 is one of the most famous and well-studied quasars. We have been studying this source intensively with VLBI, using both ground and space-based VLBI observations. Results from our collaborative VLBI Space Observatory Programme (VSOP) monitoring observations are presented by Hirabayashi et al. in these proceedings. This paper presents results from high-frequency 22 and 43 GHz ground-based VLBI observations conducted between 1991 and 1997. The earlier observations (1991–1994) were conducted with the global VLBI network and partial Very Long Baseline Array (VLBA); later observations (1994–1997) were conducted with the full VLBA. Observations at 43 GHz did not begin until 1995. We have recorded a total of 18 epochs of observation at 22 GHz between 1991 and 1997, and 10 epochs at 43 GHz between 1995 and 1997. Sample images of 3C 279 at 22 and 43 GHz are shown in Figure 1.

## 2 Components and Speeds

A total of eight components (named C4, C5, C5a, C6, C7, C7a, C8, and C9) have been identified and tracked by model fitting. These component

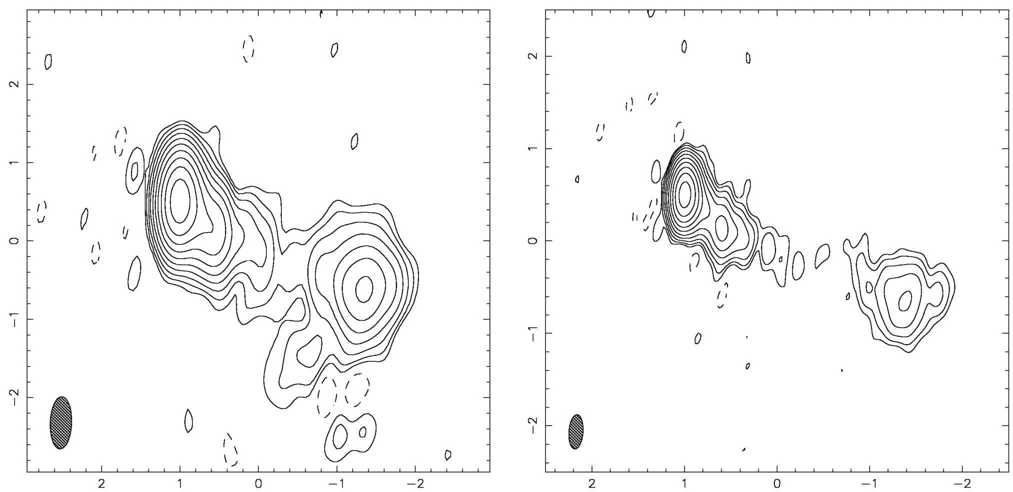

Figure 1: 22 GHz (left) and 43 GHz (right) images of 3C 279 from 1995 Mar 19. The peak flux densities are 12.3 and 13.6 Jy beam$^{-1}$, the contour levels are 15 and 18 mJy beam$^{-1}$ $\times$ -1,1,2,4,...512, and the beam sizes are 0.67 $\times$ 0.27 mas at -2° and 0.37 $\times$ 0.15 mas at -4° for the 22 and 43 GHz images respectively.

names have been chosen to maintain consistency with the C5, C6, and C7 of Leppänen et al. (1995) and the C8 of Lister et al. (1998). The outward motion of these components is shown in Figure 2. The bright component C4 currently at ~3 mas has been extremely long lived, with an ejection time in the mid 1980s. The component C5 at ~1 mas is stationary, and other superluminal components interior to C5 fade and disappear as they approach C5. The bright component C8 (which was as bright as 9 Jy) was ejected near the time of the EGRET flare in early 1996, although the formal ejection time is several sigma before the flare. Component speeds measured by fitting to component separations vs. time are ($H_0$=70 km s$^{-1}$ Mpc$^{-1}$ and $q_0$=0.1): 7.5 $\pm$ 0.2 $c$ for C4, $-0.6 \pm 0.5$ $c$ for C5, 6.8 $\pm$ 1.0 $c$ for C5a, 5.8 $\pm$ 0.4 $c$ for C6, 5.0 $\pm$ 0.4 $c$ for C7, 4.8 $\pm$ 0.2 $c$ for C7a, and 5.4 $\pm$ 0.2 $c$ for C8.

## 3 3-Dimensional Motion of C4

Component C4 has followed a nonlinear path out from the core, and we use this path and the apparent speed of C4 to model the 3-dimensional trajectory of this component, using the method described by Zensus et al. (1995) for 3C345. Polynomials were fit to $x(t)$ and $y(t)$ (Figure 3$a$).

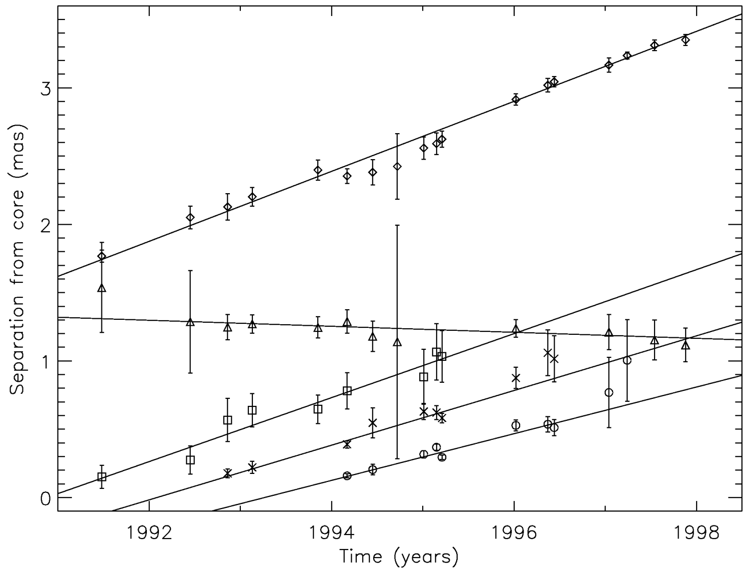


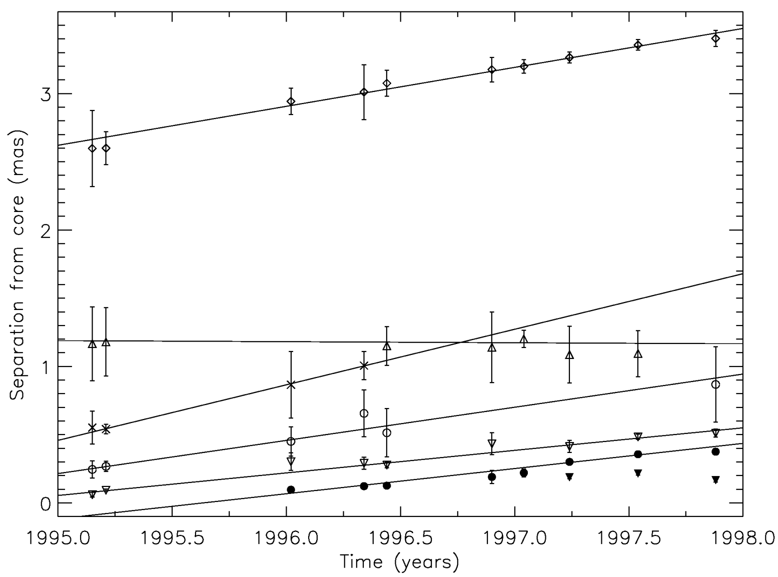


Figure 2: Distances from the core of model components as a function of time at 22 GHz (top) and 43 GHz (bottom). Diamonds represent C4, triangles C5, squares C5a, crosses C6, circles C7, inverted triangles C7a, filled circles C8, and filled inverted triangles C9. Error bars have been set to be proportional to the beam size and inversely proportional to the square root of the component SNR (component surface brightness/ rms surface brightness). The lines shown are the best fits to motion with constant speed.

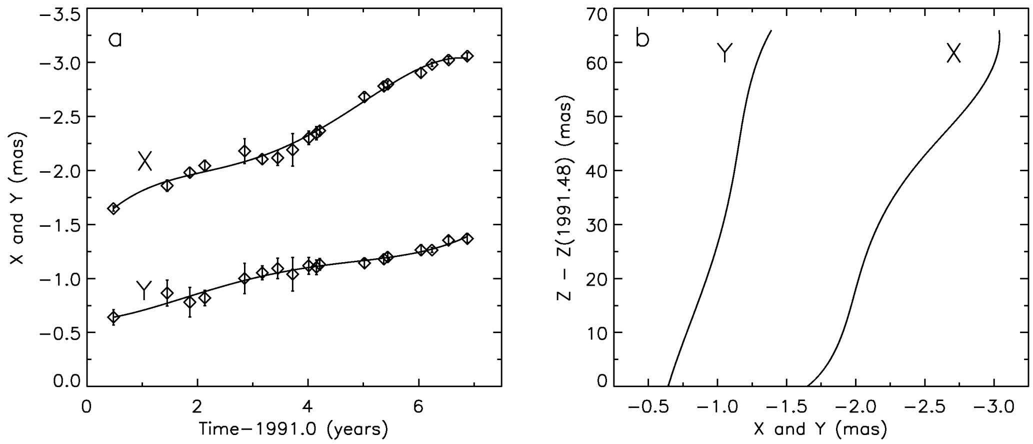


Figure 3: ($a$): $x$ and $y$ position of C4 vs. time. The lines show polynomial fits to the motion. ($b$): Derived motion of C4 in the $(x, z)$ and $(y, z)$ planes.

Fourth order polynomials were required for adequate fits. The apparent speed was found from $\beta_{app}(t) = (\dot{x}(t)^2 + \dot{y}(t)^2)^{1/2}$, and a constant $\Gamma$ slightly larger than the minimum $\Gamma$ required for the maximum $\beta_{app}(t)$ was assumed ($\Gamma = 13$). The viewing angle was then solved for, taking the small angle solution because the large angle solution gives large changes in Doppler factor that would be seen as large changes in flux. From the viewing angle, $z(t)$ can be calculated and the complete 3D trajectory determined. The motion in the $(x, z)$ and $(y, z)$ planes is shown in Figure 3$b$. C4 appears to follow a low pitch angle helical path in the $(x, z)$ plane.

**Acknowledgements.** Part of the work described in this paper has been carried out at the Jet Propulsion Laboratory, California Institute of Technology, under contract with the National Aeronautics and Space Administration. A.E.W. acknowledges support from the NASA Long Term Space Astrophysics Program. The National Radio Astronomy Observatory is a facility of the National Science Foundation operated under cooperative agreement by Associated Universities, Inc.

## References

Leppänen, K.J., Zensus, J.A., & Diamond, P.J. 1995, *AJ*, **110**, 2479

Lister, M.L., Marscher, A.P., & Gear, W.K. 1998, *ApJ*, **504**, 702

Zensus, J.A., Cohen, M.H., & Unwin, S.C. 1995, *ApJ*, **443**, 35